

TENSIONAL STATE ACTIVATED BY NOSE GEAR OF THE AIRBUS 380-800

by:

Enzo Bonvino * and **Umberto Bonvino** **

* Civil engineer of transports

** Airport Infrastructures Professor, Bari Polytechnic
ITALY

Phone: (+39) 080 5963382; Fax: (+39) 080 5963329

umbertobonvino@gmail.com

bonvino@poliba.it

PRESENTED FOR THE
2010 FAA WORLDWIDE AIRPORT TECHNOLOGY TRANSFER CONFERENCE
Atlantic City, New Jersey, USA

April 2010

INTRODUCTION

The airport pavement project requires, in general, the mass of the critical take-off aircraft; particularly it uses the load transmitted by one of the main landing rear gears; in fact the contemporary presence of two main gears on the same slab is rare. The anterior or secondary gear has essentially directional functions and it is not considered in the calculation because the load that transmits to the aircraft pavement is negligible. In this research, instead, the anterior gear of the Airbus 380 (nicknamed Super Jumbo) is examined. The Airbus A380 have all the typologies of landing gear with which the modern commercial aircrafts are equipped: directional anterior twin wheels (Nose Landing Gear - NLG), rear double tandem bearing wheels (Wing Landing Gear - WLG) and rear tridem bearing wheels (Body Landing Gear - BLG). Through a computational code FEM (Finite Element Analysis) and the predisposition of numerous models, we show that, for particular conditions of static load, the NLG, often neglected in the airport pavement design, determines tensile stress more elevated than those activated by the bearing rear gears WLG and BLG.

LOADING CONDITIONS

The recent introduction into commercial service of heavier and heavier aircrafts has highlighted the need for new advanced design methods on the airport pavements using advanced computer technology. As aircraft landing gears continue to get heavier and more complex, it has become increasingly clear that the traditional design models well known to engineers are oversimplified and inadequate to assess the effects of the new aircraft on the airport design. For rigid pavements the problem is very important; an example is constituted by the new A380 (first test flight: April 27, 2005) jewel of the Airbus Industries. The scientific literature does not much dwell on the stress-strain state produced in runways by aircraft front landing gears, while it emphasizes the magnitude of the loads transmitted by the bearing gears. On modern commercial aircraft the rear gears, in fact, transmit 90% of the aircraft's weight to the runway slab.

In this research the study of the interactions between the pavement and all the A380 landing gears is developed; in particular, it shows that the A380 NLG, while loading on the pavement only around 7% of the total load of the aircraft, plays a non secondary role in static runway design. In fact, for particular load positions, the nose gear can generate a more severe stress state than that generated by the main gears. The A380 landing gear is comprised of five gears (Fig.1); two rear pairs: tridem (Body Landing Gear) and double tandem (Wing Landing Gear), and one twin wheel front landing gear (Nose Landing Gear). Each of the two body gear stresses the pavement with a static vertical load (V_{BG}) exceeding 168 tons - the total mass of a Boeing 767-200ER on take-off. The load transmitted by the nose gear equals the maximum take-off weight (MTOW) of the DC9-21 or of a Boeing 737-100. And finally, each gear produces quite different effects depending on the position on the slab.

According to the builder's technical data, a large number of load conditions were formulated, assuming a square slab: side between 700 and 730 cm with a thickness of 40 cm. Assuming that each slab is physically independent of its fellows (no load transfer capability at the joint), the load transmitted by the isolated gears was studied. In order to get the worst-case stress characteristics the following schemes were prepared, characterized both by the position of each gear relative to the slab and by the aircraft's direction of movement. The linear analysis was conducted for those numerous positions (Cy, By, Bx, Ay, A45) and along those particular directions that were deemed important to achieving the purposes of the study (Figure 1).

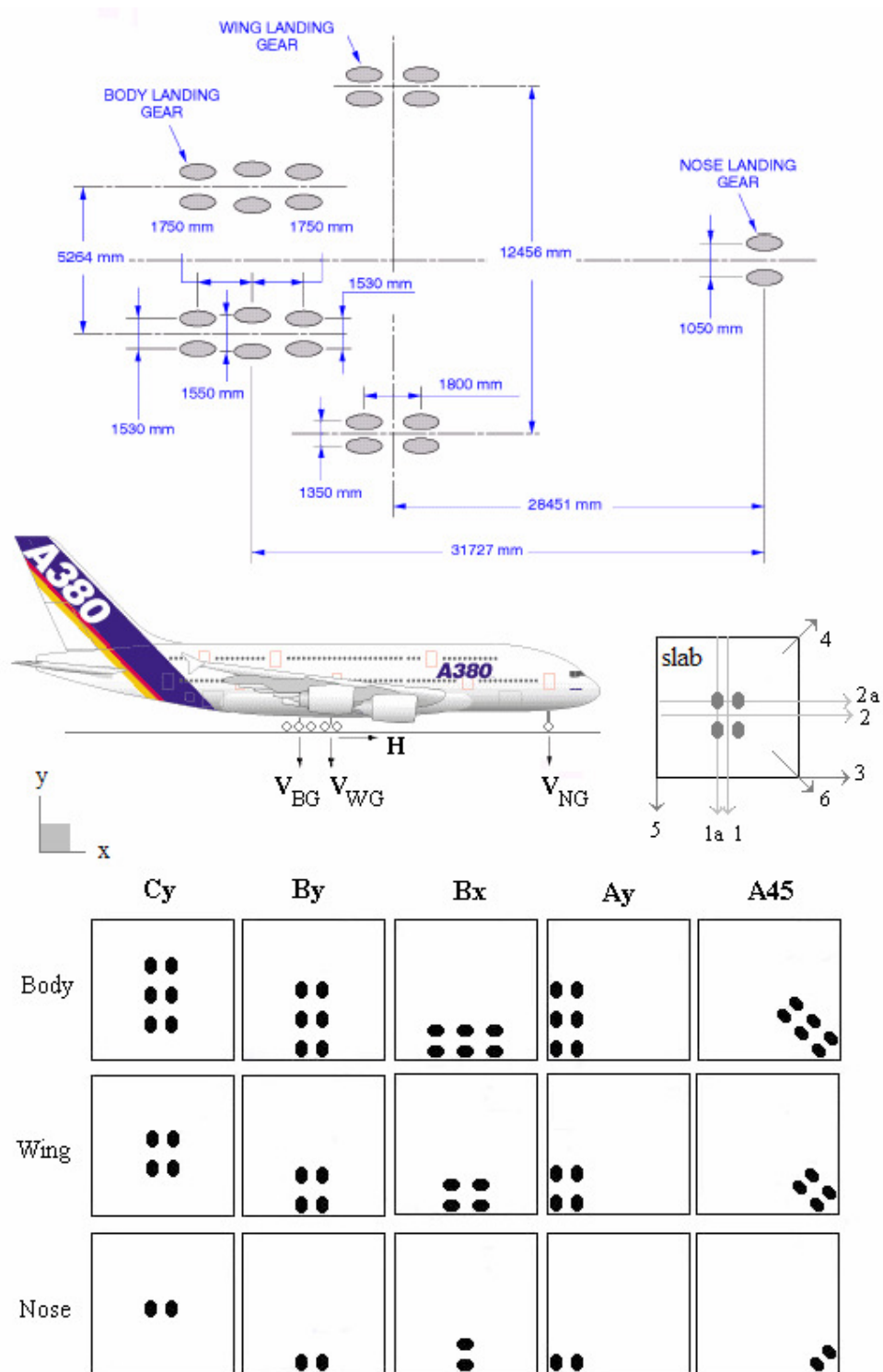


Figure 1 - Loading cases of the landing gears and reference axes (not to scale)

THE FEM MODEL

One of the advantages of the model FEM is that it allows the load to be represented with the landing gears located in any position relative to the slab. The complex and scantily reliable calculation of the equivalent single weight load (ESWL) is thus forsaken. Table 1 shows the characteristics of the rigid pavement and of the subgrade support used in this study.

Table 1.

Layer	Material	Thickness cm	Rck daN/cm ²	E daN/cm ²	ν	K daN/cm ³
Slab	Cement concrete	40	400	349.660	0,15	-
Subbase	Treated base	20	150	85.000	0,20	-
Subgrade	A ₃ /A ₄ (UNI 10006)	200	-	-	0,40	variable

Technical information on the airplane was obtained from Airbus Industries. In the calculations we assumed elliptical footprints uniformly loading the pavement. This last assumption, thought not rigorous scientifically speaking, speeded up calculation of the numerous loading cases. In this way we moved as closely as possible to the conditions underlying prof. Westergaard's hypothesis. Finally, the load on the tire imprints was assigned by means of the nodal forces, obtained using the tributary areas method. The use of materials assumed to be linear, elastic and isotropic, further reduced computing times. Nonetheless, the use of the less complex models did not produce calculations out of line with the objectives of the study which was aimed most especially at the analysis of the stress-strain state induced in the pavement by each loading typology. A mesh was prepared for each of the various gear positions, the meshes of course being denser around the areas of application of the loads and connected through special zones of transition to the area of less-dense mesh (Figure 2). During the experimentation we observed that the models could be made up using 2D elements as well, if provided with high bending rigidity and a variable stress state within the slab thickness. The differing mesh densities meant the calculation times varied considerably from area to area. Since among the study objectives was the analysis of cement concrete slab behaviour under varying loading configurations, it was deemed best to use 2D elements, which did not invalidate comparison and involved relatively short computing times. Special attention was thus given to the construction of the models, whose geometries were created respecting a number of guidelines based on a greater thickening of the radially graduated meshes around the loading zones, those deemed most stressed, and on the creation of regular elements having form ratios near to unity (except for a few elements far from the applied load). Different models resulted, each created with thousands of nodes; this meant the solution of tens of thousands of equations for each position of the gears on the pavement, and thus computation times even of hours, with a sizeable occupation of the central processor's memory.

For each of the loading configurations the following were determined: the principal normal stress σ_{11} and σ_{22} on the slab bottom and top faces, the principal unit strains ϵ_{11} and ϵ_{22} , the normal displacements along the Z-axis (\perp to the slab's median plane XY), the bending moments M_{xx} , M_{yy} , M_{xy} , curvatures, reactions. As indicators of the goodness of the models were chosen, for each loading combination and for each of the quantities above, the normalized jumps values (the jump is the maximum difference in the nodal values at each node). Note that the highest values were always less than 10%. This is reassuring as to the proper makeup of the models, which were purposely made up without resorting to load transfer through the joints. This choice was suggested essentially for time reasons: an increase in the number of elements, in fact, indispensable to the introduction of the adjacent slabs, makes computing time increase exponentially. On the other hand the joint-free modelling has its own physical significance, since it can serve for analyzing the behaviour of a loaded slab, isolated from its fellows and constrained only by the underlying

substrate. This is a convenient situation in the case where low load transmission onto unreinforced joints is neglected.

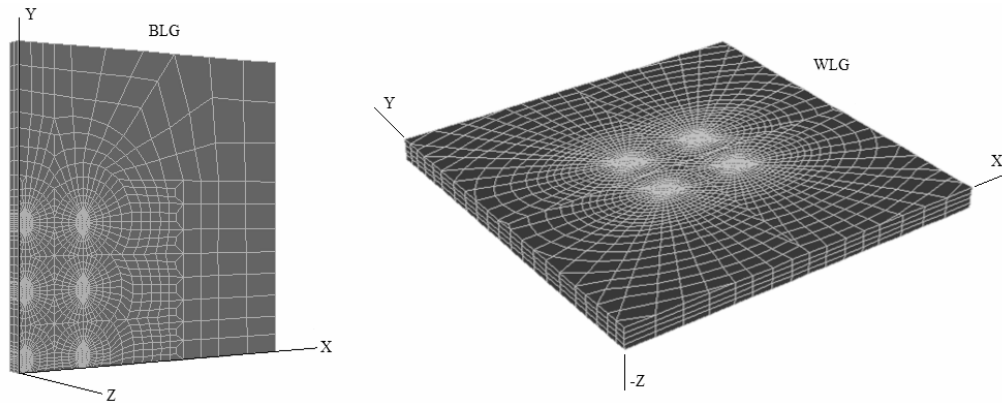


Figure 2 – Mesh. Ay and Cy configurations.

STRESS-STRAIN ANALYSIS

In order to better compare the pavement behaviour under the loads of the three types of landing gear, some computation results were visualized in different figures (Figs.3, 4, 5, 6 and 7) which show the principal stresses on both faces of the slab (upper and lower) and the vertical strain in various directions. Figure 3 shows the behaviour of the principal tensile stresses on the slab lower face along 1a direction, parallel to the y-axis, joining the centres of gravity of the imprint areas of the left wheels. Study of Figure 3 brings out the followings facts:

- The peak tensile stresses are always located in the imprint centres, whatever be the gear type.
- The stress-growth gradients from the unloaded edge up to the first wheel appear similar for all three landing gear types.
- Below the centre body gear wheel the peak tensile stress exceeds by about 6% the analogous, equal, stresses below the two outermost wheels. This characteristic, even if of different magnitude, was already seen when examining the landing gear of other aircraft having tridem gears, such as the Boeing 777 and Tupolev 154.
- The Wing gear displays, for obvious symmetry reasons, two equal stress maxima, which are slightly lower than that induced by the central body wheel.
- The stress curve produced by the Nose gear obviously displays a single peak, whose value is 23% less than that generated by the centre body wheel.
- Among the landing gears, the maximum and minimum principal stresses lie in the ratio of 1.6 for the tridem and of 1.5 for the dual tandem.

The study of the strains (Fig.3) permits the following remarks:

- In the chosen direction the slab is always strained along the z-axis, whatever be the gear involved, and this for the usual reasons due to load symmetry.
- The maximum strain is found along the slab axis of symmetry with the peak value generated by the wing gear, which exceeds by 15% and 50% those caused by the loads due to the body and the wing gears.

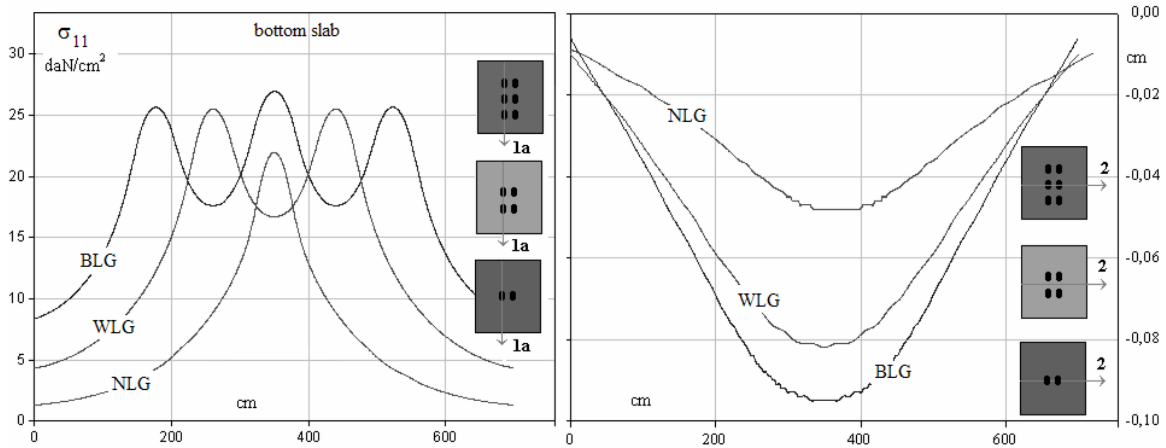


Figure 3 – Main stresses (bottom slab) and vertical displacements. Cy configuration.

Figure 4 shows the behaviour of the principal stresses on upper face; we observe:

- In the direction 1a the slab is in tensile and compression, whatever be the gear acting.
- The peak tensile is found when the nose gear, the lightest, acts on the slab; its tensile stresses exceed by 1.6 times those generated by the wing gear and by three times those induced by the body gear.
- Beneath the imprints the tridem body generates three compression peaks, the dual tandem wing two, and the nose gear of course but one maximum.
- All compression stresses appear to be small.

Finally, Figure 4 shows also for the usual three load types the stress behaviour along direction 3, coinciding with the slab’s loaded edge. In particular, inspection of the stress pattern on the slab lower face brings out:

- Along direction 3 the slab is wholly in tensile.
- The $(\sigma_{11})_{max}$ tensile stresses quite high beneath the imprints, and they vary slightly even when the gear varies.
- It is the wing gear that stresses the pavement more than the others, exceeding the principal stresses induced by the body and nose gears by 14% and 19% respectively.
- In this loading scheme too the stresses brought about by the lightest landing gear are comparable with those produced by the principal gears.

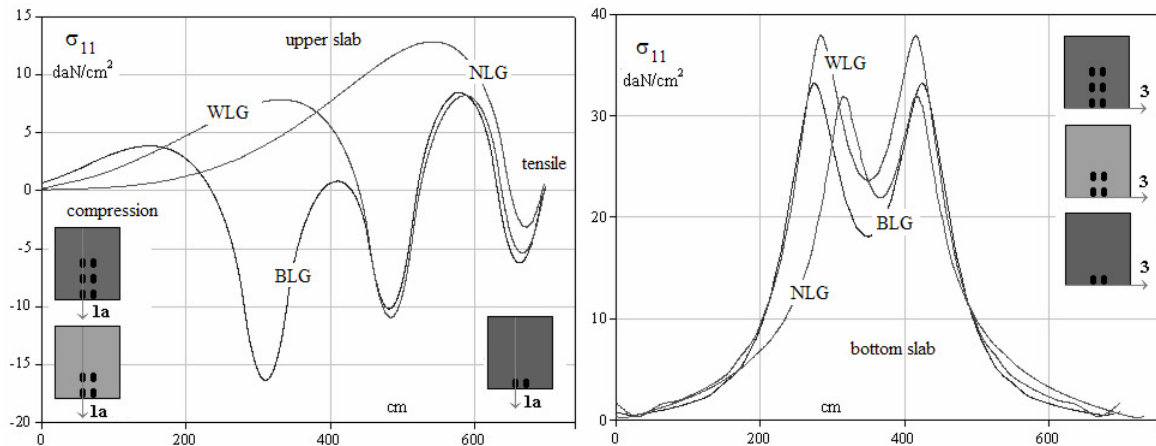


Figure 4 – Main stresses By configuration.

Figure 5 shows the stress along the direction 3 and 1. Along direction 3:

- The slab is always in tensile whatever the type of load.
- The highest values are found when the nose gear acts; they decrease slightly inferior under the load of the dual tandem wing gear and more accentuated if the body tridem is acting.
- The absolute and relative maxima are always located below the imprints areas; in particularly the three tensile peaks generated by the body gear indicate a minimum below the centre wheel, unlike what was observed under the Cy load condition. The peaks generated along the edge of the slab by the wing gear's two wheels are, of course, equal.

Along direction 1:

- The slab is all in tensile and the maximum stress is usually found nearby the loaded edge. The twin-wheel gear is surely the most critical for the pavement; along direction 1 the departures between the maximum stresses induced by the nose, wing and body gears are more obvious than was observed at first.
- The behaviour of the stresses generated by the nose gear can be described as a function that grows rapidly when the load is close to the edge; in practice, at a distance of about 1.50 m from the loaded edge the tensile stresses take on the same peak values as those induced by the body landing gear.

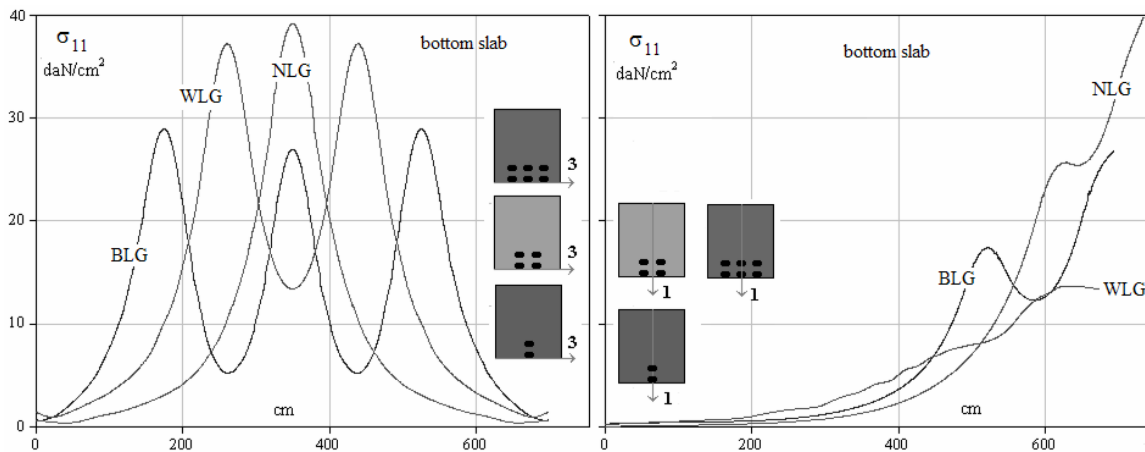


Figure 5 – Main stresses. Bx configuration

Figure 6 shows the behaviour of the principal stresses along the direction 3.

Bottom slab:

- The slab lower face is wholly under tensile for all gear locations.
- The maximum tensile stress, provided by the nose gear innermost wheel, exceeds by 31% that generated by the wing dual tandem and by 100% that generated by the body tridem.
- The tensile peaks below the wheel located on the corner of the slab too have the same sequence: the highest value belongs to the nose wheel, followed in order by the wing and body gears (respectively 18% and 88% greater).

On the slab upper face, in that same direction 3, is observed that:

- The slab is always under tensile and the maximum principal stresses differ slightly from one another depending on the landing gear acting; the highest value is achieved, still once again, by the nose gear, followed by the wing and then the body.

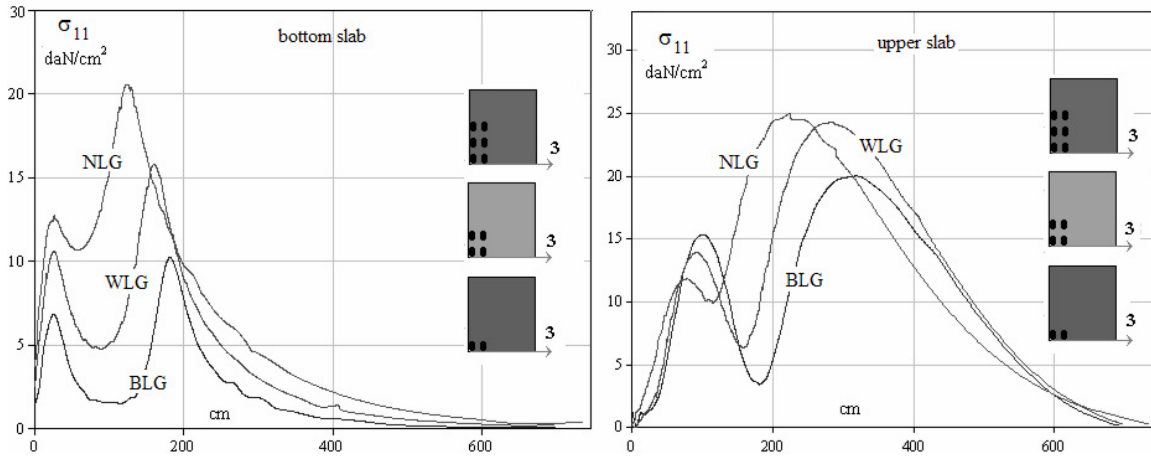


Figure 6 – Main stresses. Ay configuration.

Loading condition A45 (Figure 7) is quite complex; it therefore demands that particular directions be assumed, for example direction 6 (upper slab):

- When loaded by any one of the three gears, the slab appears to go into both tensile and compression; in general, the peak tensile values exceed those found on the lower face only below the nose gear. This characteristic is not found with the other landing gears.
- The absolute maximum tensile stress is induced by the nose gear; its numerical value definitely exceeds that induced by the other heavier gears. This tensile is achieved nearby the twin wheels, towards the interior of the slab.
- Below the imprint areas of the two wheels closest to the slab's loaded corner there is a slight tensile when the load is induced by the principal gears: body and wing; the nose gear instead generates a moderate compressions.

Figure 7 shows also the vertical strains in direction 6:

- The strain absolute values increase as the loaded corner is approached.
- The maximum strain is found below the wheels of the nose and wing gears.
- Only for body loading is there observed a very slight lifting of the unloaded corner of the slab.

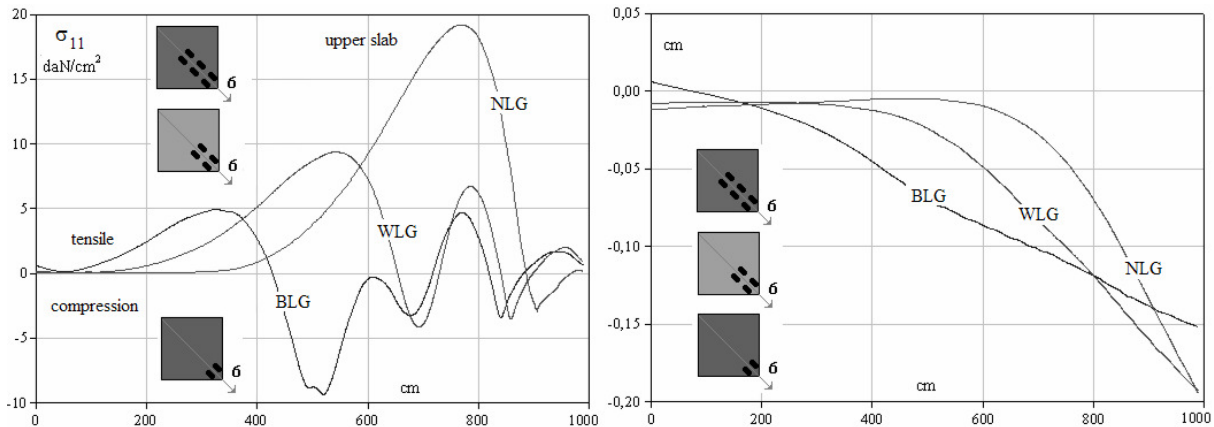


Figure 7 – Main stresses (upper slab) and vertical displacements. A45 configuration.

The analysis of the results was completed with the 3D representation of the vertical strains induced by some of the load conditions considered earlier. In particular, Figure 8 shows in order the slab loaded by the isolated body, wing and nose gears bearing on a corner (A45 configuration).

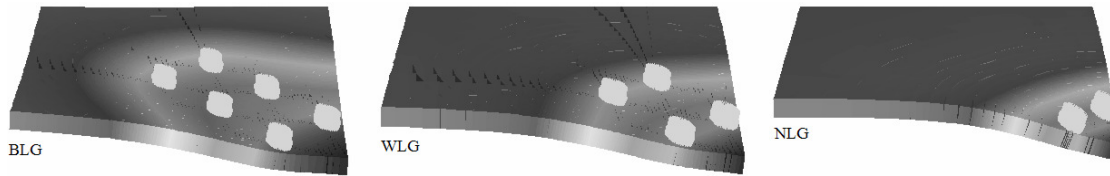


Figure 8 – 3D displacements. A45 configuration.

CONCLUSIONS

It has been shown that on cement-concrete airport pavements the loads transmitted by the principal wheels of the gigantic Airbus 380 do not always bring about the maximum stresses. The geometry of the landing gears (with special emphasis on the size of the gauge) and the tyre pressures are the parameters that most influence the magnitude of the tensile stresses and of the strains when we consider only one subgrade support and we assume that joints do not transfer the load. All this means that when designing new runways or taxiways where the critical aircraft is the super Jumbo, greater use must be made of more in-depth calculation methods and, most especially, very high standards for the quality of the materials forming the pavement must be applied. The A380 landing gears were placed according to particular configurations in such fashion as to simulate the worst-case loading conditions for a concrete slab. In this study it was noted that for some of these schemes the front landing gear (nose gear) while applying only 7% of the weight of the entire aircraft, brings about the highest tensile stresses.

To complete this work the two schemes of Figure 9 were made up. These summarize, for varying load conditions and Airbus 380 landing gear types, the location of the wheels below which appear the principal tensile stresses (on the slab lower face) and the highest vertical strains. Finally, in order to cluster the results got from the experiments carried out on the three landing gear types, Figure 10 ($K=10 \text{ daN/cm}^3$) was made up, which shows the normalized ratios of the stresses (on both slab faces) and of the vertical strains. Reference values are those of the centred loading scheme (Cy), induced by the heaviest gear (body gear). It is to be observed that the nose gear in loading scheme By (lower and upper face), Bx (lower and upper face), Ay (upper face) and A45 (upper face), generates stresses exceeding those generated by the body gear in the centred-load configuration. In the Bx (lower face), By (upper face), Ay (upper face) and A45 (upper face) schemes, the σ_{11} tensile caused by the front gear exceed those induced by any principal landing gear. Finally, with regard to strains, the Ay and A45 schemes associated with the nose gear furnish numerical values exceeding those got by the heaviest gear in Cy configuration.

The FEM analysis brings out the excellent distribution of the loads exerted by the body gear, whose proper design makes it possible for each of its six wheels to stress the pavement independently of one another. For some load configurations, in order to alleviate the high stress regime it would be best to outfit the wing gear with six wheels and not with a dual tandem.

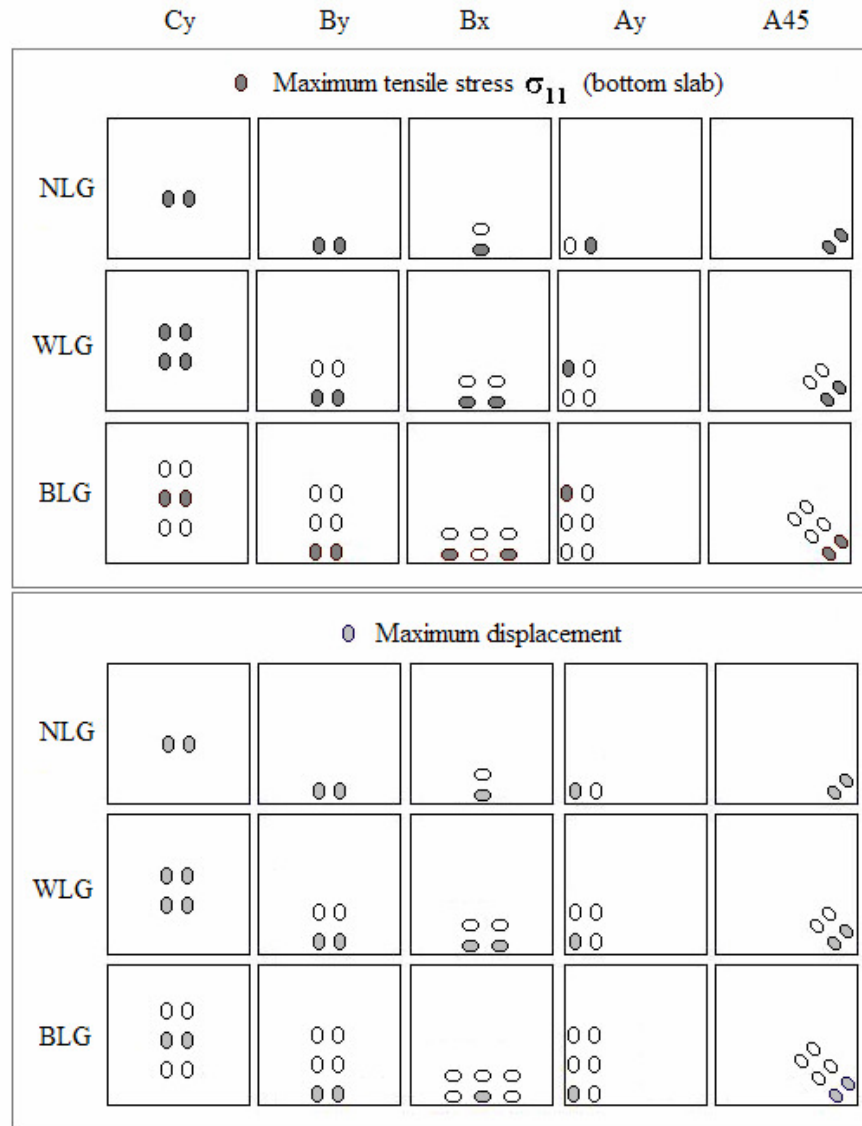


Figure 9 – The location of the $(\sigma_{11})_{max}$ and maximum displacements for every loading case.

The variations of the subgrade support (K) do not change the previous comparison between the landing gears. Obviously, the reduction of K determines increases in tensile stresses as shown in Table 2. Major changes are always referred to WLG. Whatever the intensity of the subgrade support, the NLG provides in Bx configuration the maximum value of principal tensile stresses.

Table 2. Variation of tensile stresses (%).

Bx configuration			
bottom slab - direction: 1a			
K daN/cm ³	BLG	WLG	NLG
10	100,0	100,0	100,0
8	102,7	106,4	104,6
6	109,6	114,9	110,1
4	123,9	126,7	117,6

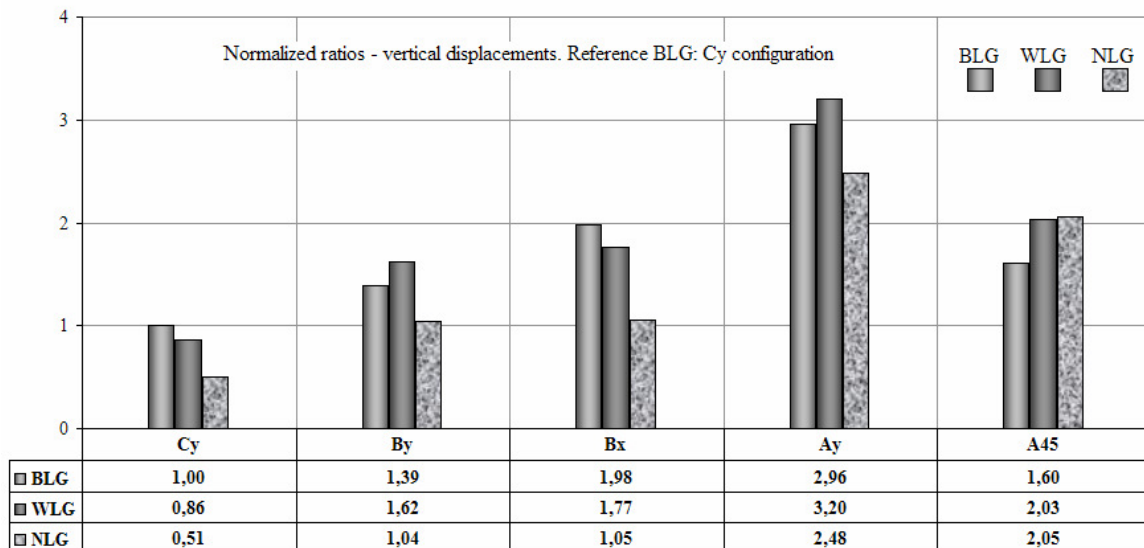
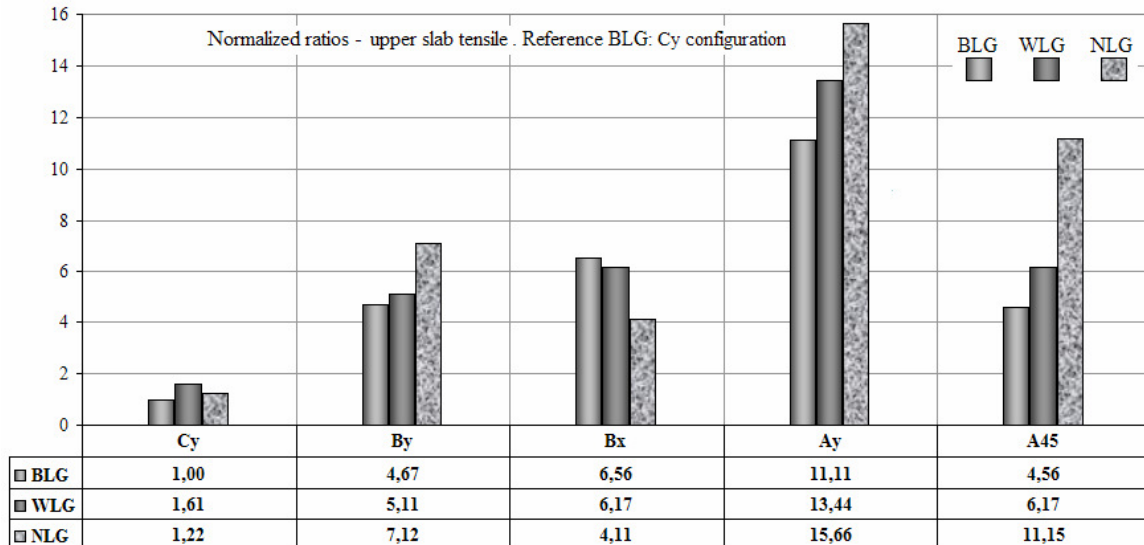
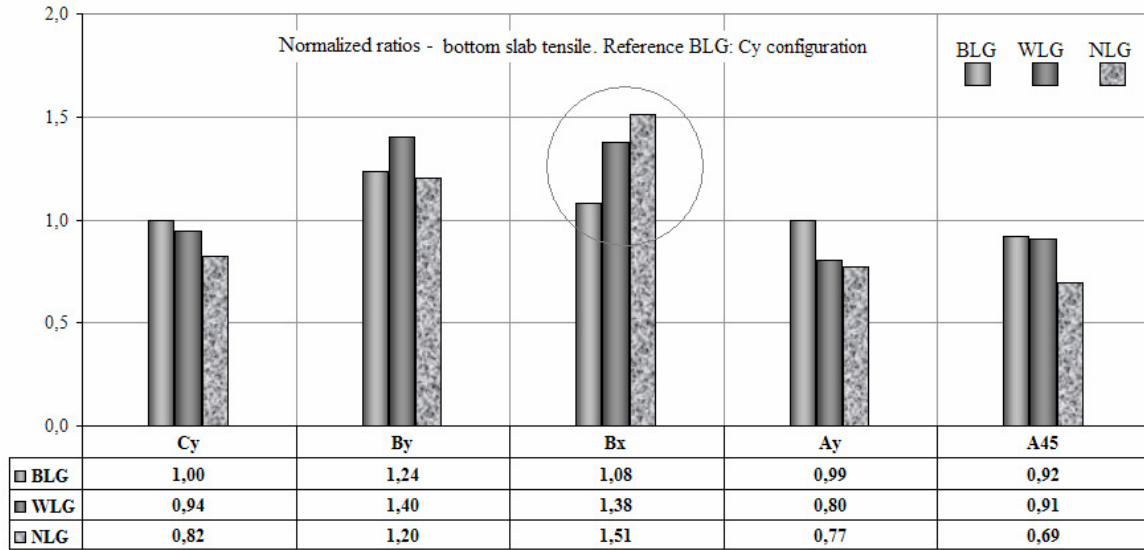


Figure 10 - Normalized ratios: tensile stress and vertical deformations.

REFERENCES

1. Bonvino Enzo & Bonvino Umberto. *L'età dei Jet. Dal Comet alla Città volante*. Aracne Editore. Roma. Pag.781. 2006
2. Bonvino Enzo and Bonvino Umberto. "The runway length for the take-off of the largest airplane of the world: the Airbus 380. FAA Worldwide Airport Technology Transfer Conference. Atlantic City, New Jersey, USA. 2004
3. Bonvino Umberto. "*La pista di volo. La geometria*". 2° Edizione. Editore Arti Grafiche Favia. Bari (Italia). Pag.308. 2009
4. Bonvino Umberto. "*Dizionario Aeronautico*". Editore Arti Grafiche Favia. Bari (Italia). 2007. Formato elettronico.
5. Internet: various sites. Just examples: Airliners.net, Air04.it, Airliners.net, air-and-space.com, allstar.fiu.edu, Aeromedia.it, avia-dejavu.net, aviation-fr.info, aviation-safety.net, classic-aircraft.oldclassicar.co.uk, discovery-italia.com/flight/jet_planes/, ecplanet.com , Flugrevue.rotor.com, hq.nasa.gov, jp4.it, Newton.com, Surf.to/Comet, US Air Force, Wikipedia.org, Airbus.com, Boeing.com, ecc.
6. Manual and company website Airbus Industrie.
7. Westergaard, H.M., "New Formulas for Stresses in Concrete Pavements of Airfields," *Transactions*, ASCE, Vol. 108, pp. 831-856, 1948.
8. Westergaard, H.M., "Om Beregning af Plader paa elastik Underlag med saerlight paa Sporgsmaalet om Spaendinger I Betonveje". *Ingeniøren* Vol.32, n.42. 1923.
9. Westergaard, H.M., "Stresses in concrete pavements computed by theoretical analysys". *Public Roads* 7. 1926.
10. Bonvino Umberto & Bonvino Enzo. "*La pista di volo. La sovrastruttura*". Editore Arti Grafiche Favia. Bari (Italia). Pag.397. 2010.

The Authors declare to have contributed fairly to the preparation of this study.